Inorg. Chem. **2005**, *44*, 3283–3289

Characterization of the Low-Energy Electronic Excited States of Benzoyl-Substituted Ruthenocenes

Cynthia T. Sanderson, Jessica A. Quinlan, Richard C. Conover, Michael K. Johnson, Michael Murphy, Richard A. Dluhy, and Charles Kutal*

Department of Chemistry, University of Georgia, Athens, Georgia 30602

Received December 17, 2004

Electronic absorption and resonance Raman spectral studies of benzoylruthenocene (BRc) and 1,1′-dibenzoylruthenocene (DRc) indicate that the low-energy electronic excited states of these 4d^6 metallocenes possess metal-to-ligand charge transfer (MLCT) character. While this MLCT contribution should weaken the metal-ring bonding in the excited state, neither compound is photosensitive in nonhalogenated solvents such as methanol, acetonitrile, and cyclohexane. In contrast, irradiating BRc and DRc in the good electron-accepting solvent, carbon tetrachloride, results in ring loss via a pathway that appears to originate from a charge-transfer-to-solvent excited state. Both metallocenes function as photoinitiators for the anionic polymerization of ethyl 2-cyanoacrylate, and the kinetics and mechanism of this process have been investigated. Comparing the present results on BRc and DRc with those reported earlier for the corresponding benzoyl-substituted ferrocene compounds reveals some interesting commonalities and differences between the excited-state properties of these 3d and 4d metallocenes.

Introduction

Adding substituents to a molecule may alter the nature of its low-lying electronic excited states with profound consequences on spectral and photochemical properties. Our recent studies of Group 8 metallocenes provide an example of such behavior. We reported that ferrocene and ruthenocene (Fc and Rc, respectively, in Figure 1) function as photoinitiators for the anionic polymerization of ethyl 2-cyanoacrylate (CA).[1] Detailed examination of this process revealed that it occurs by an intermolecular charge-transfer pathway involving the initial formation of a ground state donor−acceptor complex between the electron-rich metallocene and the electrophilic monomer (shown for Fc in eq 1). Irradiation of the complex at wavelengths that populate a metallocene → CA charge-transfer-to-solvent (CTTS) excited-state triggers a redox reaction that yields the corresponding metallocenium cation and the monomer radical anion. It is this latter species that initiates anionic polymerization by addition to the C=C double bond of CA.

$$\mathrm{Fc} + \mathrm{CA} \rightleftharpoons \underset{\text{donor-acceptor complex}}{[\mathrm{Fc}\cdot\cdot\mathrm{CA}]} \xrightarrow{h\nu} \mathrm{Fc}^{+} + \mathrm{CA}^{\cdot-} \qquad (1)$$

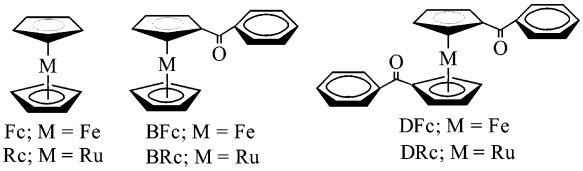

Figure 1. Structures and abbreviations for the Group 8 metallocenes discussed in the text.

Photoinitiation occurs by a completely different mechanism for benzoylferrocene and 1,1′-dibenzoylferrocene (BFc and DFc, respectively, in Figure 1).[2−4] The presence of the electron-withdrawing benzoyl substituent on one or both cyclopentadienyl rings introduces metal-to-ligand charge transfer (MLCT) character into the low-energy electronic excited states of these metallocenes. This intramolecular charge-transfer contribution, which can be represented by a resonance structure of the type shown for DFc in Figure 2, formally reduces the hapticity of a cyclopentadienyl ring from η^5 to η^4 and enhances the susceptibility of the metal center to nucleophilic attack by solvent. Both effects facilitate heterolytic metal-ring bond cleavage to yield the half-

* Address correspondence to this author. E-mail: ckutal@chem.uga.edu; fax: (706) 542-9454.

(1) Sanderson, C. T.; Palmer, B. J.; Morgan, A.; Murphy, M.; Dluhy, R. A.; Mize, T.; Amster, I. J.; Kutal, C. *Macromolecules* **2002**, *35*, 9648−9652.
(2) Yamaguchi, Y.; Kutal, C. *Inorg. Chem.* **1999**, *38*, 4861−4867.
(3) Yamaguchi, Y.; Kutal, C. *Macromolecules* **2000**, *33*, 1152−1156.
(4) Ding, W.; Sanderson, C. T.; Conover, R. C.; Johnson, M. K.; Amster, I. J.; Kutal, C. *Inorg. Chem.* **2003**, *42*, 1532−1537.

10.1021/ic0482178 CCC: $30.25
Published on Web 04/07/2005

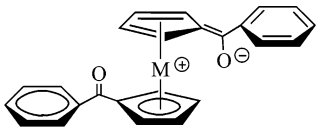

Figure 2. Resonance structure depicting the MLCT character of the low-energy electronic excited states of benzoyl-substituted Group 8 metallocenes. Formal charges on atoms are circled.

sandwich iron compound and a benzoylcyclopentadienide anion (eq 2, S is solvent). The liberated anion is a potent initiator for the polymerization of CA.

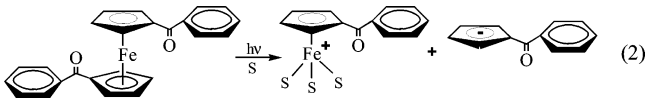

(2)

This duality in the mechanism of photoinitiation by ferrocene compounds arises from the different orbital characters (CTTS vs MLCT) of the electronic excited states that generate the initiating species. In this Article, we examine whether similar behavior occurs within the corresponding series of ruthenium-containing metallocenes. Studies of the spectral, photochemical, and photoinitiation properties of benzoylruthenocene and 1,1′-dibenzoylruthenocene (BRc and DRc, respectively, in Figure 1) have yielded information pertinent to the following related questions. (1) Do benzoyl substituents introduce MLCT character into the low-energy electronic excited states of these ruthenocene derivatives? (2) Do BRc and DRc undergo photoinduced heterolytic metal-ring bond cleavage analogous to eq 2? (3) Do BRc and DRc function as photoinitiators for the anionic polymerization of CA? (4) If photoinitiation does occur, what mechanism is involved? Comparison of the present results with those found earlier for ferrocene compounds have revealed some interesting parallels and contrasts between the excited-state properties of related $3d^6$ and $4d^6$ metallocenes.

Experimental Procedures

Reagents. Ferrocene (Aldrich) and ruthenocene (Strem) were sublimed prior to use, while 1,1′-dibenzoylferrocene (Sigma) was recrystallized from warm *n*-hexane. A mixture of benzoylruthenocene and 1,1′-dibenzoylruthenocene was prepared by published procedures.[5,6] The crude product was dissolved in dichloromethane and separated into its components by column chromatography on silica gel. Elution with CH_2Cl_2 yielded BRc, after which elution with a 5:95 (by volume) mixture of acetonitrile/CH_2Cl_2 gave DRc. Following the removal of solvent by rotary evaporation, BRc was recrystallized from warm *n*-hexanes, and DRc was recrystallized from a warm 1:1:13 (by volume) mixture of benzene/petroleum ether/*n*-hexanes. The solid products were dried overnight in a vacuum desiccator. Anal. Calcd for $C_{24}H_{18}O_2Ru$ (DRc): C, 65.58; H, 4.14. Found: C, 65.54; H, 4.15. mp 124−124.5 °C. Calcd for $C_{17}H_{14}ORu$ (BRc): C, 60.88; H, 4.22. Found: C, 60.91; H, 4.13. mp 125.5−126.2 °C. Solvents used in the spectral and photochemical studies were at least reagent-grade quality and used as received from the supplier.

Instrumentation and Procedures. Melting points were determined with a Thomas−Hoover Unimelt apparatus and are uncorrected. Electronic absorption spectra were recorded at room temperature (23 ± 3 °C) on a Cary 300 spectrophotometer. Continuous photolysis experiments were performed with an Illumination Industries 200-W high-pressure mercury arc lamp. Polychromatic light of wavelengths >290 nm was obtained by passing the full output of the lamp through Pyrex glass.

Raman spectra were recorded using an Instruments SA Ramanor U1000 spectrometer fitted with a cooled RCA-31034 photomultiplier tube. Spectra were recorded digitally using photon counting electronics, and improvements in the signal-to-noise ratio were achieved by signal averaging multiple scans. Absolute band positions were calibrated using the excitation frequency and CCl_4 and are accurate to ± 1 cm^{-1}. Lines from a Coherent Innova 200-K2 krypton ion laser were used for excitation, and plasma lines were removed using a Pellin Broca prism pre-monochromator. Scattering was collected from the surface of the sample using 90° scattering geometry and a custom-designed sample cell,[7] which was attached to the coldfinger of an Air Products Displex Model CSA-202E closed cycle refrigerator maintained at 17 K. Solid-state spectra were recorded using samples prepared as KBr disks, containing 2% (w/w) K_2SO_4 as an internal standard, and the disks were attached to the surface of the sample holder using Crycon grease. The time course of the effect of laser exposure on Raman intensity of discrete bands was monitored by optimizing alignment using the sulfate band, blocking the laser beam, adjusting the position of the sample so that the focused laser beam hit a different spot on the surface of the sample, initiating a time-based scan at a fixed frequency, and simultaneously unblocking the laser beam at time zero.

Photolyzed solutions were analyzed by electrospray ionization mass spectrometry (ESI−MS) operated in the positive ion mode. In one set of experiments, acetonitrile solutions of BRc or DRc were irradiated offline in a 1 cm rectangular quartz spectrophotometer cell. One mL aliquots of the photolytes were diluted to 10 mL with acetonitrile that had been refluxed over and distilled from calcium hydride, and sodium iodide (10-fold molar excess relative to ruthenium) was added as a cation carrier. Sample solutions were passed through a 0.2 μm syringe filter before being injected into a Mariner Biospectrometry Workstation (PerSeptive Biosystems, Inc.), which combines a time-of-flight mass spectrometer with an electrospray source. Details of the instrumental setup and typical operating parameters are provided in a recent Article.[8] In another experiment, a solution of BRc dissolved in carbon tetrachloride turned cloudy upon irradiation (similar behavior occurred for DRc). A brown precipitate was filtered off, washed with cyclohexane, and dried in a desiccator. Elemental analysis of this material yielded the following result: C, 36.99; H, 3.20. The solid was washed with acetonitrile before being dissolved in 88% formic acid. Aliquots of the original carbon tetrachloride filtrate, the acetonitrile washings, and the precipitate dissolved in formic acid were diluted 1:99 (v:v) with acetonitrile and analyzed on a Sciex Atmospheric Pressure Ionization I-Plus quadrupole mass spectrometer (Perkin-Elmer).

Photoinitiated polymerization of CA was monitored by attenuated total reflectance Fourier transform infrared spectroscopy (ATR−

(5) Rausch, M. D.; Fischer, E. O.; Grubert, H. *J. Am. Chem. Soc.* **1960**, *82*, 76−82.
(6) LeMay, G.; Kaliaguine, S.; Adnot, A.; Nahar, S.; Cozak, D.; Monnier, J. *Can. J. Chem.* **1986**, *64*, 1943−1948.
(7) Drozdzewski, P. M.; Johnson, M. K. *Appl. Spectrosc.* **1988**, *42*, 1575−1577.
(8) Ding, W.; Johnson, K. A.; Kutal, C.; Amster, I. J. *Anal. Chem.* **2003**, *75*, 4624−4630.

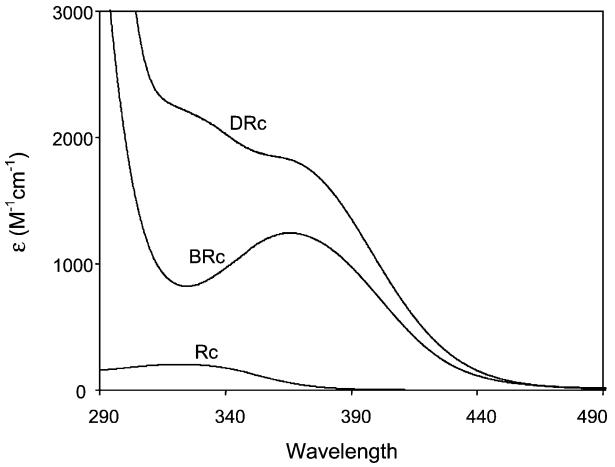

Figure 3. Electronic absorption spectra of ruthenocene (Rc), benzoylruthenocene (BRc), and 1,1′-dibenzoylruthenocene (DRc) in room-temperature methanol.

FTIR) with Bio Rad FTS-60 and FTS-7000 spectrometers equipped with a narrow band HgCdTe detector. A small strip of sample solution containing a metallocene dissolved in neat monomer was applied to a germanium ATR crystal mounted in a horizontal ATR accessory (CIC Photonics) within the sample chamber of the spectrometer. Assuming a refractive index of 1.5 for CA and 4.0 for Ge, and a 45° angle of incidence, we calculated that the electric field of the monitoring IR beam penetrated the sample to a depth of 2−3 μm.[9] Polymerization commenced upon irradiating the sample with the polychromatic output of the mercury-arc lamp. Incident light intensity was measured with a Coherent Radiation Model-10 power meter. For samples containing Rc, BRc, or DRc, infrared absorbance spectra were collected every second using the following parameters: three co-added scans, triangular apodization with one level of zero filling, and a 4 cm^{-1} resolution. For samples containing Fc or DFc, one co-added scan was collected every 1.5 s. Spectra were analyzed with the Grams 32/AI spectral software package (Galactic Industries). Peak heights, frequencies, and areas were calculated with a center-of-gravity algorithm[10] using a program written by R. A. Dluhy. The area of the C═O stretching band of CA at 1734 cm^{-1} was assumed to remain constant during polymerization and used as an internal standard to correct the area of the C═C stretching band at 1616 cm^{-1} for changes in sample thickness.

Results and Discussion

Electronic Absorption Spectral Studies. The electronic absorption spectra of Rc, BRc, and DRc in room-temperature methanol are compared in Figure 3. The parent metallocene, Rc, exhibits a single band above 300 nm that contains contributions from two unresolved ligand field transitions ($^1A_{1'} \rightarrow {}^1E_{1'},{}^1E_{2'}$ in D_{5h} symmetry).[11] The low intensity of the band reflects the Laporte-forbidden d−d character of these transitions. Consistent with the metal-localized nature of ligand field transitions, the band undergoes only minor changes in position and intensity as a function of solvent polarity.

Table 1. Solvent Dependence of the Electronic Absorption Spectrum of BRc

solvent	dielectric constant[a]	λ_{max}, nm[b]	e_{max}, $M^{-1}\,cm^{-1}$
methanol	32.7	365	1250
acetonitrile	37.5	356	977
cyclohexane	2.02	342	1020
carbon tetrachloride	2.24	345	1320
chloroform	4.81	358	1340

[a] Data from ref 27. [b] Maximum of low-energy absorption band.

Adding a benzoyl group to one or both rings of Rc causes dramatic changes in spectral properties. As seen in Figure 3, BRc and DRc exhibit absorption bands at longer wavelengths and with significantly higher intensities than the parent metallocene. Moreover, the positions of these bands exhibit a dependence on solvent polarity[12] as exemplified by the data for BRc in Table 1. Such behavior is incompatible with a pure ligand field assignment for these bands. Instead, we propose that the electron-withdrawing benzoyl substituent mixes metal-to-ligand charge-transfer character into the low-energy electronic excited states of BRc and DRc. Representing this MLCT contribution by a resonance structure of the type shown in Figure 2 emphasizes the charge separation that occurs upon photoexcitation. Coulombic stabilization of this dipolar excited state by the surrounding medium influences its energy relative to the ground state, thus accounting for the dependence of band maxima on solvent polarity. In addition, mixing MLCT character into the electronic transitions of BRc and DRc relaxes the Laporte selection rule and thereby enhances band intensities.

Previous studies have shown that Rc can form a ground state donor-acceptor complex with a good electron-accepting solvent.[13,14] In carbon tetrachloride, for example, this complex is characterized by a Rc $\rightarrow$ CCl_4 CTTS absorption band that appears in the near-ultraviolet region. We investigated whether this type of donor−acceptor behavior also occurs with the benzoyl-substituted ruthenocenes. Spectral data were obtained for BRc (Table 1; DRc behaves similarly) in a series of solvents whose electron-accepting ability follows the order carbon tetrachloride > chloroform > cyclohexane. While band positions are sensitive to changes in solvent, no feature attributable to a CTTS transition is evident above 300 nm in the spectra measured in the halogenated media. Instead, the spectra vary in a manner that correlates reasonably well with solvent polarity. Thus, the low-energy band occurs at very similar wavelengths in the nonpolar solvents, cyclohexane and carbon tetrachloride, but shifts to lower energy in the more polar chloroform. We conclude from these results that CTTS transitions of benzoyl-substituted ruthenocenes in halogenated solvents occur at relatively high energy and are effectively masked by the more intense metallocene bands containing MLCT character.

Resonance Raman Studies. Further evidence that the low-energy electronic absorption bands of BRc and DRc contain

(9) Harrick, N. J. *Internal Reflection Spectroscopy*; Harrick Scientific Corp.: Ossining, NY, 1979; p 30.
(10) Cameron, D. G.; Moffat, D. J.; Mantsch, H. H. *Appl. Spectrosc.* **1983**, *36*, 245−249.
(11) Sohn, Y. S.; Hendrickson, D. N.; Gray, H. B. *J. Am. Chem. Soc.* **1971**, *93*, 3603−3612.
(12) We adopt dielectric constant as a convenient measure of solvent polarity.
(13) Traverso, O.; Sostero, S.; Mazzochin, G. A. *Inorg. Chim. Acta* **1974**, *11*, 237−241.
(14) Borrell, P.; Henderson, E. *J. Chem. Soc., Dalton Trans.* **1975**, 432−438.

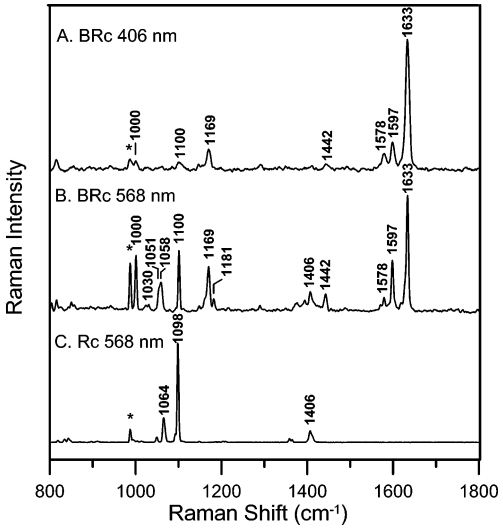

Figure 4. Low-temperature (17 K) Raman spectra of Rc and BRc. Samples were prepared as KBr disks (8% (w/w) Rc or BRc and 2% (w/w) K_2SO_4). The spectra of Rc and BRc obtained with 568 nm excitation were collected with a 170 mW laser power at the sample and are the sum of 45 scans with each scan involving photon counting for 1 s every 1 cm^{-1} using a 5 cm^{-1} resolution. The spectrum of BRc obtained with 406 nm excitation was collected with a 30 mW laser power at the sample and is the sum of 33 scans with each scan involving photon counting for 1 s every 1 cm^{-1} using a 6 cm^{-1} resolution. The asterisk marks the sulfate band at 985 cm^{-1}, which is used as an internal standard for the extent of resonance enhancement.

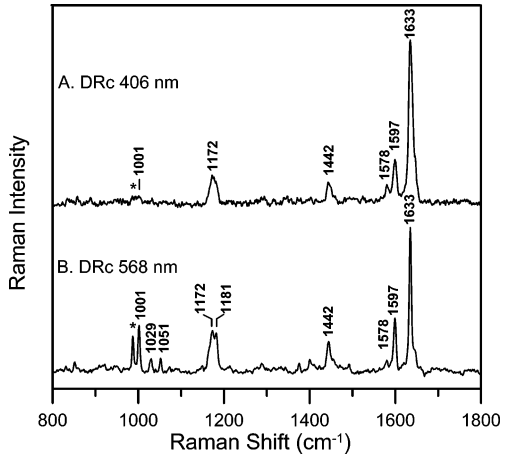

Figure 5. Low-temperature (17 K) Raman spectra of DRc. The sample was prepared as a KBr disk (8% (w/w) DRc and 2% (w/w) K_2SO_4). The conditions of measurement using 568 and 406 nm excitation were the same as those described in Figure 4. The asterisk marks the sulfate band at 985 cm^{-1}, which is used as an internal standard for the extent of resonance enhancement.

MLCT character was provided by resonance Raman spectroscopy. Charge-transfer transitions are particularly effective for inducing resonant enhancement of the Raman-active vibrational modes of chromophores when the excitation frequency lies within the absorption envelope. Moreover, to a first approximation, resonant enhancement is generally most pronounced for vibrations that mimic the distortion in the electronic excited state.[15] Referring to the excited-state resonance structure shown in Figure 2, we expect that excitation into the low-energy absorption bands of BRc and DRc should cause selective enhancement of in-plane vibrations of the cyclopentadienyl and phenyl rings owing to changes in conjugation between the two rings, as well as strong enhancement of the carbonyl vibrational mode due to lengthening of the C−O bond. This expectation is fully confirmed by the low-temperature (17 K) solid-state Raman spectra of Rc and BRc shown in Figure 4 and of DRc shown in Figure 5. Table 2 contains the vibrational assignments of the dominant bands, which are based on published assignments.[4,16,17] The Raman spectra of Rc obtained with 568 and 406 nm excitation were identical, with individual bands exhibiting the same relative intensities to each other and the sulfate internal standard, as expected for spontaneous rather than resonance Raman scattering. In contrast, the relative intensities of the Raman bands observed for BRc and DRc change dramatically with respect to each other and the sulfate internal standard for spectra obtained using nonresonant (568 nm) and resonant (406 nm) excitation. For both of these benzoyl-substituted ruthenocenes, the vibrations of the benzoylcyclopentadienyl ligand are enhanced relative to the sulfate internal standard using 406 nm excitation, with the greatest enhancement for the C−O stretching mode at 1633 cm^{-1}, whereas the vibrations of the unsubstituted cyclopentadienyl ring in BRc are not significantly enhanced.

Table 2. Vibrational Frequencies (cm^{-1}) and Assignments in the Resonance Raman Spectra of Rc, BRc, and DRc

Rc	BRc	DRc	assignment[a]
	1633	1633	ν(CO)
	1597	1597	$\nu(CC)_{Ph}$
	1578	1578	$\nu(CC)_{Ph}$
	1442	1442	$\nu(CC)_{Cp'}$
1406	1406		$\nu(CC)_{Cp}$
	1181	1181	$\delta(CCH)_{Ph}$ or $\delta(CCH)_{Cp'}$
	1169	1172	$\delta(CCH)_{Ph}$ or $\delta(CCH)_{Cp'}$
1098	1100		$\nu(CC)_{Cp}$
1064	1058		$\delta(CCH)_{Cp}$
	1051	1051	$\delta(CCH)_{Cp'}$
	1030	1029	$\nu(CC)_{Ph}$
	1000	1001	$\delta(CCC)_{Ph}$

[a] Ph is phenyl; Cp and Cp′ denote unsubstituted and benzoyl-substituted cyclopentadienyl rings, respectively.

The Raman results obtained herein for BRc and DRc are very similar to those previously reported for BFc and DFc using nonresonant (647 nm) and resonant (568 nm) excitation.[4] In contrast to BFc and DFc, for which photoinduced loss of the benzoylcyclopentadienide anion occurred using laser excitation at 568 nm into the low-energy tail of the MLCT band, no evidence for laser-induced photodegradation of BRc or DRc was evident using 406 nm excitation into the low-energy tail of the MLCT band. Indeed, no change in the Raman intensity for the dominant band at 1633 cm^{-1} was observed over a 10 min period following exposure to the laser beam. Hence, both BRc and DRc are much less susceptible to photolytic metal-ring bond cleavage than their BFc and DFc counterparts. This conclusion is supported by the photochemical results reported in the following section.

(15) Spiro, T. G.; Czernuszewicz, R. S. In *Physical Methods in Bioinorganic Chemistry: Spectroscopy and Magnetism*; Que, L., Jr., Ed.; University Science Books: Sausalito, CA, 2000; pp 59−120.
(16) Bodenheimer, J. S.; Low, W. *Spectrochim. Acta* **1973**, *29A*, 1733−1743.
(17) Nakamoto, K. *Infrared and Raman Spectra of Inorganic and Coordination Compounds*, 5th ed.; John Wiley and Sons: New York, 1997.

Photochemical Studies. While Fc and Rc are photoinert in nonhalogenated solvents such as acetonitrile and methanol, BFc and DFc undergo photoinduced metal-ring bond cleavage (eq 2) in these media. The disparate behavior exhibited by the two sets of compounds has been attributed to the mixing of MLCT character into the low-energy electronic excited states of the benzoyl-substituted ferrocenes. As seen from the resonance structure in Figure 2, this MLCT contribution facilitates ligand photosubstitution by weakening metal-ring bonding and enhancing the susceptibility of the metal to attack by solvent.

Having established that the low-energy excited states of BRc and DRc possess this type of MLCT character, we examined whether these 4d metallocenes are prone to photoinduced ring loss. Acetonitrile solutions of each compound, some of which had been deoxygenated by bubbling with argon, were irradiated for 30 min with the Pyrex-filtered output of a 200-W high-pressure mercury lamp. In all cases, the electronic absorption spectrum of the photolyte was unchanged from that of a dark control sample. Similar results were obtained upon irradiating the metallocenes in methanol or cyclohexane. Assuming that a 5% reaction could be detected by this technique, we calculate that the quantum efficiency for ring loss from the benzoyl-substituted ruthenocenes is $<4 \times 10^{-4}$. This surprising lack of photoreactivity was confirmed in another set of experiments that employed electrospray ionization mass spectrometry to analyze samples. No peaks attributable to half-sandwich compounds or other photoproducts were observed in the ESI mass spectra of acetonitrile solutions of the metallocenes that had been irradiated for 20−30 min. Collectively, our results indicate that BRc and DRc are photoinert in nonhalogenated solvents.

We also investigated the photochemical behavior of carbon tetrachloride solutions of BRc and DRc. Samples irradiated for 10−20 min turned cloudy and deposited a fine brown precipitate. ESI−MS analysis of the filtrates and, in the case of BRc, the acetonitrile used to wash the precipitate and a formic acid solution of the precipitate revealed the presence of small amounts (<5% relative abundance) of species such as $[(\eta^5\text{-}C_5H_5)Ru(CH_3CN)]^+$ and $[(\eta^5\text{-}C_5H_4C(O)C_6H_5)Ru(CH_3CN)_2]^+$.[18] Formation of these half-sandwich products indicates that photoinduced ring loss occurred in the halogenated solvent.[19]

Photoinitiation Studies. Solutions of CA containing millimolar concentrations of Fc, DFc, Rc, BRc, or DRc polymerize to a hard, plastic-like solid when irradiated with white light. Qualitative observations reveal that the time required for solidification varies widely within this group of metallocene photoinitiators. Samples containing Rc or DFc solidify within seconds with the evolution of a considerable quantity of heat. In contrast, samples containing Fc generally require much longer irradiation times, during which the initially nonviscous liquid thickens to a syrupy consistency. Solidification of this material then occurs over a 2−3 h period of storage in the dark.

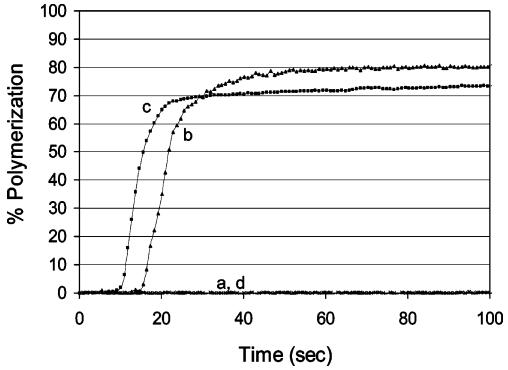

Figure 6. Plots of percent polymerization vs time for samples of CA containing 10.0 mM Rc: (a) nonirradiated, (b) irradiated with 33 mW/cm^2 polychromatic light, (c) irradiated with 117 mW/cm^2 polychromatic light, and (d) irradiated with 117 mW/cm^2 polychromatic light after the addition of 133 ppm methanesulfonic acid.

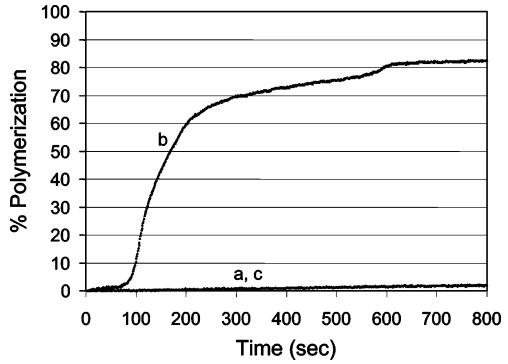

Figure 7. Plots of percent polymerization vs time for samples of CA containing 11.6 mM DRc: (a) nonirradiated, (b) irradiated with 105 mW/cm^2 polychromatic light, and (c) irradiated with 105 mW/cm^2 polychromatic light after addition of 113 ppm methanesulfonic acid.

Quantitative characterization of photoinitiated polymerization was obtained by attenuated total reflectance Fourier transform infrared spectroscopy. This technique allows real-time monitoring of the polymerization occurring in a 2−3 μm layer of monomer immediately adjacent to the surface of the ATR crystal. The extent of polymerization is directly related to the decrease in the absorbance of the C=C stretching band of CA at 1616 cm^{-1}. This relationship is defined by eq 3, where A_o denotes the initial (dark) area of the band and A_t is the area after irradiation for time t. Representative plots of percent polymerization versus irradiation time are displayed in Figures 6 and 7 for samples of neat CA containing Rc or DRc, respectively. Plots with very similar characteristics were obtained for the other metallocene photoinitiators tested. Typically, polymerization exhibits an induction period that depends on light intensity (compare curves b and c in Figure 6) and the quantum efficiency of generating the active initiating species. Thereafter, polymerization accelerates rapidly before finally approaching a plateau at 75−85% conversion. We attribute the induction period to the presence in the commercial monomer

(18) The coordinatively unsaturated ruthenocene species detected by ESI−MS (e.g., four-coordinate $[(\eta^5\text{-}C_5H_5)Ru(CH_3CN)]^+$) most likely results from collision-induced dissociation of acetonitrile from the initially formed photoproduct (e.g., $[(\eta^5\text{-}C_5H_5)Ru(CH_3CN)_3]^+$) after the latter species exits the ESI tip. For further information about this process, see Ding, W.; Johnson, K. A.; Amster, I. J.; Kutal. C. *Inorg. Chem.* **2001**, *40*, 6865−6866.

(19) The low carbon content of the precipitate is consistent with the formation of ring-loss photoproducts.

Table 3. Rate (R_p) Data for Photoinitiated Polymerization of CA

photoinitiator	concentration, mM	light intensity, mW/cm^2	R_p, M/s[a]
Fc	9.6	110	0.060
DFc	2.7	30	1.7
Rc	10.0	33	0.56
Rc	10.0	117	0.94
BRc	10.5	126	0.68
DRc	11.6	105	0.14

[a] Maximum rate calculated from eq 4.

of an acid stabilizer, which serves as a scavenger for adventitious traces of basic impurities. Polymerization is inhibited until sufficient anionic species are photochemically generated to neutralize this acid, whereupon rapid consumption of monomer commences. Consistent with this interpretation, the addition of extra acid to a sample lengthens the induction period (compare curves b and c in Figure 7) and slows the ensuing anionic polymerization.

$$\% \text{ polymerization} = \frac{A_o - A_t}{A_o} \times 100 \qquad (3)$$

The rate of photoinitiated polymerization, R_p, at any point during a run can be determined by using eq 4, where A_{t1} and A_{t2} represent the areas of the 1616 cm^{-1} band at the indicated times, and M is the molar concentration of vinyl groups in the monomer. To establish a common benchmark for making comparisons, we calculated the maximum rate attained with each photoinitiator during the acceleratory period of the polymerization process. These data, which are compiled in Table 3, reveal two contrasting trends. First, for the ferrocene compounds, R_p decreases in the order DFc > Fc, indicating that the presence of a benzoyl group has a salutary effect on the rate of photoinitiated polymerization.[20] This result agrees with prior observations that CA solutions containing DFc or BFc require shorter irradiation times to undergo a visually detectable change in viscosity than solutions containing Fc.[21] Second, the benzoyl group has the exact opposite effect within the ruthenocene series, with R_p decreasing in the order Rc > BRc > DRc. Possible reasons for this interesting reversal in the trends of R_p values for corresponding 3d^6 and 4d^6 metallocene photoinitiators will be considered in the following section.

$$R_p = \frac{M(A_{t1} - A_{t2})}{A_o(t_2 - t_1)} \qquad (4)$$

Mechanistic Considerations. Evidence obtained from electronic absorption and resonance Raman spectroscopic studies strongly supports the conclusion that irradiation of BRc and DRc with visible light (e.g., 406 nm) populates excited states containing MLCT character. Accordingly, the limiting resonance structure shown in Figure 2 provides a qualitatively useful description of the charge distribution in these states. While the MLCT contribution should weaken metal-ring bonding, irradiation of BRc or DRc in nonhalogenated media such as methanol and acetonitrile does not result in the efficient heterolytic metal-ring bond cleavage observed for the corresponding benzoyl-substituted ferrocenes (eq 2). This photoinertness correlates with the greater ground-state metal-ring bond strength of 4d versus 3d metallocenes,[22] suggesting that the photoexcited ruthenocene compounds retain sufficient bonding to prevent ring loss. Moreover, the residual bonding in the excited state may be enhanced by η^6-fulvene coordination of the labilized ring as depicted in Figure 8.[23] This coordination mode should be more important in BRc and DRc than in the corresponding ferrocenes owing to the greater radial extension of 4d versus 3d orbitals and the resulting better overlap with the exocyclic double bond of the fulvene moiety.

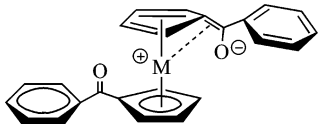

Figure 8. Resonance structure depicting η^6-fulvene bonding of the labilized ring in the low-energy electronic excited states of benzoyl-substituted Group 8 metallocenes. Formal charges on atoms are circled.

Switching the solvent to carbon tetrachloride or CA turns on the photoreactivity of the benzoyl-substituted ruthenocenes. While we have not detected a distinct CTTS band in the absorption spectra of the metallocenes in these electron-accepting media, it appears reasonable to assign metallocene → solvent charge transfer as the primary photochemical event leading to the final products. Kinetic evidence consistent with this assignment is presented in Table 3, which shows that the maximum rate of photoinitiated CA polymerization decreases in the order Rc > BRc > DRc. Importantly, the metal center in the metallocene becomes increasingly difficult to oxidize in the same order owing to the electron-withdrawing effect of the benzoyl group.[24] This correlation between photoinitiation and redox properties is consistent with a mechanism whereby photoinduced metallocene → CA electron transfer generates the active initiating species, which, by analogy to eq 1, is assigned as the CA radical anion.

It was noted in the previous section that 3d^6 and 4d^6 metallocene photoinitiators for the anionic polymerization of CA exhibit opposite responses to the presence of the benzoyl group. We can now understand this behavior in terms of the competition between the two charge-transfer-induced pathways that yield the active initiating species: intermolecular metallocene → CA electron transfer versus intramolecular heterolytic metal-ring bond cleavage. Electron-rich Fc favors the former pathway, while BFc and DFc prefer the latter. The observed trend in the maximum rates of photoinitiated polymerization, DFc > BFc > Fc, can be understood in terms of two contributing factors. First, the MLCT bands of BFc and DFc possess higher molar absorptivities and extend over a broader wavelength range than the

(20) The difference in the R_p values for the two metallocenes would have been even larger had comparable light intensities been used.
(21) Yamaguchi, Y.; Palmer, B. J.; Kutal, C.; Wakamatsu, T.; Yang, D. B. *Macromolecules* **1998**, *31*, 5155−5157.
(22) Long, N. J. *Metallocenes: An Introduction to Sandwich Complexes*; Blackwell Science: London, 1998; Ch. 4.
(23) Barlow, S.; Cowley, A.; Green, J. C.; Brunker, T. J.; Hascall, T. *Organometallics* **2001**, *20*, 5351−5359.
(24) Page, J. A.; Wilkinson, G. *J. Am. Chem. Soc.* **1952**, *74*, 6149−6150.

CTTS band of the Fc···CA ground-state complex. Consequently, the benzoyl-substituted derivatives use a larger fraction of the incident radiation in forming the active initiating species. Second, the photochemical reaction that generates the initiating species occurs with higher quantum efficiency for DFc as compared to BFc.[2] While both photoinitiation pathways are available to the ruthenium-containing metallocenes, strong metal-ring bonding effectively precludes heterolytic bond cleavage. Therefore, only photoinduced metallocene → CA electron transfer is effective in generating the initiating species, and as discussed previously, the trend in the maximum rate, Rc > BRc > DRc, mirrors the ease of oxidizing the metal center.

Concluding Remarks. We posed four questions in the Introduction concerning the excited-state properties of benzoyl-substituted ruthenocenes. Brief responses to these questions are presented next, along with comparisons to the behavior of the corresponding ferrocene compounds.

(1) The benzoyl group introduces MLCT character into the low-energy electronic excited states of BRc and DRc. The spectroscopic (absorption and resonance Raman) consequences of this MLCT contribution mimic those reported earlier for BFc and DFc.

(2) Despite this MLCT contribution, neither BRc nor DRc undergoes efficient heterolytic metal-ring bond cleavage in nonhalogenated solvents such as acetonitrile and methanol. This photoinertness, which stands in contrast to the behavior of the corresponding ferrocenes, reflects the stronger metal-ring bonding and the possible contribution of η^6-fulvene coordination in the excited states of the ruthenocenes.

(3) Both BRc and DRc function as photoinitiators for the anionic polymerization of CA, although less effectively than Rc. This relative order of effectiveness is opposite to that found for the ferrocene analogues.

(4) Group 8 metallocenes undergo two photochemical reactions that generate an active initiating species for the anionic polymerization of CA: intermolecular metallocene → CA electron transfer (eq 1) and intramolecular heterolytic metal-ring bond cleavage (eq 2). BRc and DRc favor the first process, while BFc and DFc prefer the second.

Finally, the present study offers some practical guidance to those designing metallocene-(π-bridge)-acceptor molecules (metallocene = Fc or Rc) for use as second-order nonlinear optical (NLO) dyes.[25] Like the benzoyl-substituted metallocenes pictured in Figure 1, these supramolecular systems possess low-energy electronic excited states that contain MLCT character.[26] The metal-ring bond weakening that occurs in this type of excited state (Figure 2) may result in permanent ring loss, which would shorten the working life of a NLO device. Our results reveal that photoinduced metal-ring bond cleavage becomes less serious upon switching from a 3d (Fe) to a 4d (Ru) metal. Accordingly, we expect the ruthenocene-based supramolecular systems to exhibit better long-term photochemical stability.

Acknowledgment. We thank the National Science Foundation (MCB-9808857 to M.K.J.) and the National Institutes of Health (EB-001956 to R.A.D.) for financial support. Acknowledgment also is made to the donors of the Petroleum Research Fund, administered by the American Chemical Society, for support (C.K.) of this research. We greatly appreciate the assistance provided by Prof. I. J. Amster and Dr. Dennis Phillips in obtaining the mass spectral results.

IC0482178

(25) Barlow, S.; Marder, S. R. *Chem. Commun.* **2000**, 1555−1562.
(26) Barlow, S.; Bunting, H. E.; Ringham, C.; Green, J. C.; Bublitz, G. U.; Boxer, S. G.; Perry, J. W.; Marder, S. R. *J. Am. Chem. Soc.* **1999**, *121*, 3715−3723.
(27) Murov, S. L. *Handbook of Photochemistry*; Marcel Dekker: New York, 1973; pp 85−86.